Born random phase approximation for ion stopping in an arbitrarily degenerate electron fluid

G. Maynard, C. Deutsch

Classification
Physics Abstracts
52.25F — 32.70J — 52.25K

Born random phase approximation for ion stopping in an arbitrarily degenerate electron fluid

G. Maynard and C. Deutsch

Laboratoire de Physique des Gaz et des Plasmas (+), Université Paris-Sud, 91405 Orsay, France

(*Reçu le 16 novembre 1984, accepté le 8 mars 1985*)

Résumé. — Le freinage d'un ion ponctuel non relativiste par un fluide dense et homogène d'électrons est calculé en utilisant l'expression exacte de la fonction diélectrique R.P.A. ($r_s < 1$) à température arbitraire. Les résultats sont donnés en fonction de $\alpha^e = \mu/k_B T$, paramètre de dégénérescence. Des formules d'interpolations sont données permettant de regrouper les expressions asymptotiques à grande et faible vitesse respectivement. La comparaison entre la statistique de Fermi et celle de Boltzmann est faite à température quelconque. Le rapport avec d'autres approximations antérieures, basse et haute température est mis en évidence. En particulier, le calcul de Jackson ($T \to \infty$) est modifié pour minimiser l'écart avec l'approximation Born R.P.A. dans un large domaine de densité et de vitesse. L'intérêt de cette étude pour la fusion inertielle par ions lourds est mis en évidence.

Abstract. — The full R.P.A. dielectric function ($r_s < 1$) is introduced in a calculation for stopping of pointlike and nonrelativistic positive ions in a homogeneous and dense electron fluid at any temperature. Results are given for values of degeneracy $\alpha^e = \mu/k_B T$. Accurate asymptotic expressions are worked out in the small and large projectile velocity limits. Simple interpolation formulae are displayed. The replacement of Fermi statistics by Boltzmann is also investigated for any temperature. Contact is achieved with previous high- and low-temperature approximations. The Jackson limit is recovered at $T \to \infty$ and is modified in order to fit the full range of target densities and projectile velocities of interest. Relevance to heavy ion driven fusion is stressed throughout.

1. Introduction.

In close connection with beam-target interaction problems encountered in inertial confinement fusion (ICF) driven by particle beams [1-7], we intend to solve exactly the model for the stopping of nonrelativistic pointlike and positive ions in a homogeneous, and dense electron fluid taken at any temperature. Such a model is usually considered as the simplest in providing a coherent theoretical framework with reliable estimates for the beam-target interaction parameters. The rational underlying this view is based on the observation that many, if not most, of the compressed pellet states encountered during a full compression lie in the parameter space close to weakly coupled systems indexed by a dimensionless quantity

$$\chi^2 = \frac{1}{\pi q_F a_0} = \frac{V_0}{mV_F} = \frac{1}{\pi}\sqrt{\frac{I_H}{k_B T_F}} = \frac{\alpha r_s}{\pi}, \quad (1)$$

with q_F, V_F, T_F denoting Fermi wave number, velocity and temperature respectively. a_0, V_0, I_H refer to Bohr wavelength, velocity and energy $r_s = (\frac{4}{3}\pi n)^{-1/3} a_0^{-1}$ in terms of the free electron number density n, while $\alpha = (9\pi/4)^{-1/3}$. At high temperature ($T \gg T_F$), equation (1) becomes ($T_e = T/T_F$)

$$\frac{3\chi^2}{2T_e} = \frac{e^2}{\pi k_B T R_{ee}} = \frac{\Gamma_e}{\pi}, \quad (2)$$

in terms of $R_{ee} = (\frac{4}{3}\pi n)^{-1/3}$ and of the classical plasma parameter Γ_e. At any degeneracy (or temperature), the Random Phase Approximation (R.P.A.) is valid in a (T, n) domain defined by

$$\frac{\chi^2}{1 + T_e} \ll 1, \quad (3)$$

so that the potential energy content of an electron pair located at the screening distance always remains much smaller than the kinetic energy per particle. As restricted as it looks at first sight, inequality (3) allows us to encompass a huge number of different

(+) Associé au C.N.R.S.

systems ranging from high-temperature Tokomaks to dense and moderately hot plasmas envisioned in particle beam driven ICF.

Another fundamental point, stressing the basic importance of a simple but efficient modelling for the free electron component of an otherwise strongly coupled ionic mixture in the target, lies on the observation that although the bound electrons always provide a non-negligible amount to stopping, the free electrons are expected to give the largest part within the usual temperature range of interest [1, 7], i.e.

$$50 \text{ eV} < k_B T < 200 \text{ eV} .$$

Therefore, energetic ions impinging on the target are supposed to yield most of their energy to free electrons, which display more flexibility in exchanging momentum and energy during elastic collisions with projectiles. In this respect, the Born approximation is fundamental to treat the electron-ion encounter. The projectile is then considered, at variance, as pointlike, or as a quantum plane wave-packet. At last, it should be mentioned that we are fully entitled to reduce the complex beam-target interaction to a single ion-target interaction, in agreement with the fact that whatever its intensity (kiloamps up to megaamps/cm^2), any beam will appear as dilute in dense matter. The inbeam ion-ion average distance is likely to remain at least two orders of magnitude larger than the Thomas-Fermi screening length in cold matter.

The present paper is organized as follows :

— the exact R.P.A. dielectric formalism is briefly reviewed and adapted to our purposes in section 2,

— stopping calculations are performed for free electrons within R.P.A. in section 3,

— pseudoanalytic expressions as well as comparisons with previous results restricted to the high- and low-temperature domains are discussed in section 4. A certain emphasis is given to the small and large projectile velocity (V) dependence, respectively. A distinctive feature of the present approach lies in its uniformity with respect to V. Making use of a fully dynamic dielectric function allows us to compute stopping at any projectile velocity.

A preliminary account for some of these results has already been given [6, 7]; limit behaviours at high and low T, respectively, are stressed in section 5 where contact is made with previous works.

2. R.P.A. dielectric function.

We start with the usual assumption that the Coulomb interaction between a projectile and the stopping free electron is essentially elastic, so there are no such things as electron pair creation or other inelastic processes. So, we are entitled to consider the given interaction within the standard framework of linear response theory satisfying the usual relation

$$\mathbf{Jind} = -\frac{i\omega}{4\pi}(\varepsilon(q,\omega) - 1)\,\mathbf{E}(q,\omega),$$

and it remains to compute the fully dynamical dielectric function $\varepsilon(q, \omega)$. For this goal, we shall follow the exact R.P.A. treatment previously worked out by Gouedard and Deutsch [11].

2.1 GENERAL RESULTS. — They pertain to an homogeneous electron fluid which remains weakly coupled for any degeneracy

$$\frac{k_B T}{\varepsilon_F}.$$

It is the obvious finite-temperature extension of the standard Lindhard quantity valid at $T = 0$, for $r_s < 1$. It smoothly joins the $T \to \infty$ and classical Fried-Conte expressions. Within the framework of linear response theory, it is also introduced as [11].

$$\varepsilon(q,\omega) = 1 - V(q)\,X^0(q,\omega) \tag{4}$$

with

$$V(q) = \frac{4\pi e^2}{q^2}$$

and a free electron response

$$X^0(q,\omega) = -2\int \frac{dk^3}{(2\pi)^3}\,\frac{[n^0(k+q) - n^0(k)]}{[(\hbar\omega + i\eta) - (\varepsilon^0_{k+q} - \varepsilon^0_k)]} \tag{5}$$

where η is a small positive quantity,

$$\varepsilon^0_k = \frac{\hbar^2 k^2}{2 m_e},$$

$$n^0_k(k) = \{ e^{\beta[\varepsilon^0_k - \mu]} + 1 \}^{-1},$$

$$\beta = \frac{1}{k_B T}, \quad \text{and } \mu \text{ is the chemical potential}.$$

To simplify the discussion, we make use of the dimensionless variables

$$z = \frac{q}{2 q_F} \quad \text{and} \quad u = \frac{\omega}{q v_F},$$

so that

$$\begin{aligned} X^0(z,u) &= -\frac{\alpha r_s}{\pi^2}\,G(z,u) \\ G(z\ u) &= f_1(z,u) + i f_2(z,u), \end{aligned} \tag{6}$$

$$f_2(z,u) = -\frac{\pi T_e}{8z}\,\mathrm{Log}\,\frac{1 + \exp\left(\dfrac{\gamma^e - p_+^2}{T_e}\right)}{1 + \exp\left(\dfrac{\gamma^e - p_-^2}{T_e}\right)}. \tag{7}$$

The other dimensionless parameters are

$$T_e = \frac{T}{T_F}, \quad \gamma^e = \frac{\mu}{\varepsilon_F^0} = \alpha^e T_e, \quad P_\pm = u \pm z$$

$f_1(z, u)$ is computed through the Kramers-Kronig relation

$$f_1(z, u) = -\frac{1}{\pi} P \cdot P \cdot \int_{-\infty}^{+\infty} \frac{f_2(z, u')}{(u - u')} du' \tag{8}$$

which can be transformed through

$$f_1(z, u) = -\frac{\pi T_e}{8z} [F(p_+) - F(p_-)] \tag{9}$$

into

$$F(p) = -\frac{1}{\pi} P \cdot P \cdot \int_{-\infty}^{+\infty} \frac{h(p')\, dp'}{p - p'}$$

$$h(z) = \mathrm{Log}\left(1 + \exp\left[\frac{\gamma^e - z^2}{T_e}\right]\right).$$

With equations (7), (8), (9) one recovers the two well-known temperature limits :

— $T_e \ll 1$ (Lindhard [8])

$$F(p) = 2p\left[\frac{1}{2} + \frac{1 - p^2}{4p} \mathrm{Log}\frac{p + 1}{p - 1}\right] \tag{10}$$

— $T_e \gg 1$

$$F(p) = \frac{4}{3\pi T_e^{3/2}} Z(p/\sqrt{T_e}) \tag{11}$$

$Z(p)$ being the usual Fried and Conte function [9, 13]

$$Z(p) = -\frac{1}{\sqrt{\pi}} \int_{-\infty}^{+\infty} dt \frac{\exp(-t^2)}{(p - t)} \tag{12}$$

which can also be easily computed through Padé approximants [14].

At arbitrary temperatures, the following technical remarks are useful :

— f_1 and f_2 are essentially significant on a range in u (or z) measured by $a_0(T_e)$, with [11]

$$a_0(T_e) = \frac{1}{\sqrt{2}} [\gamma^e + (\gamma^{e2} + \pi^2 T_e^2)^{1/2}]^{1/2}. \tag{13}$$

The thermal velocity reads $V_{th} \simeq V_F a_0(T_e)$.

— f_1 and f_2 have their respective maxima, in u and z, located between 0 and $1/(1 + T_e)$, so

$$\chi^2 f_1(u, z) \ll a_0(T_e).$$

— $f_2(u, z) \simeq 0$ as soon as $|z - u| > 2a_0(T_e)$ (14)

— $f_1(u, z) < 0$ for $u > a_0(T_e)$.

2.2 Asymptotic expansions. — In order to check rapidly the extensive numerical calculations required in the sequel, we think it convenient to work out the following expansions :

$$\frac{\pi T_e}{2} F(p) = (2pT_e)^{1/2} \left[\frac{1}{2} F_{1/2}(\alpha^e) + \frac{p^2}{T_e} G_1(\alpha^e) + \right.$$
$$\left. + \frac{p^4}{T_e^2} G_2(\alpha^e) + \cdots\right] \tag{15}$$

for $p \ll a_0(\alpha^e)$ with α^e expressed in terms of Fermi function.

$$F_n(\alpha^e) = \int_0^\infty \frac{x^n}{(e^{x - \alpha^e} + 1)} dx$$

(computed accurately through Padé approximants [12]) as $(\frac{2}{3}) T_e^{-3/2} = F_{1/2}(\alpha^e)$, which yields the chemical potential in terms of the electron temperature and density.

$$\frac{\pi T_e}{2} F(p) = \frac{2}{3p}\left(1 + \frac{T_e}{3p^2} \frac{F_{3/2}(\alpha^e)}{F_{1/2}(\alpha^e)} + \right.$$
$$\left. + \frac{T_e^2}{5p^4} \frac{F_{5/2}(\alpha^e)}{F_{1/2}(\alpha^e)} + \cdots\right) \tag{16}$$

with $p \gg a_0(\alpha^e)$, where [10]

$$G_1(\alpha^e) = -\frac{1}{3} \int_0^\infty \frac{dx\, e^{\alpha^e - x}}{x^{1/2}(1 + e^{\alpha^e - x})^2}, \tag{17}$$

and

$$G_2(\alpha^e) = \frac{2}{15} \int_0^\infty \frac{dx}{x^{1/2}} e^{(\alpha^e - x)} \frac{(1 - e^{\alpha^e - x})}{(1 + e^{\alpha^e - x})^3} \tag{18}$$

For small z, one thus derives useful expansions such as

$$f_1(u, z) = -\frac{1}{3u^2}\left(1 + \frac{T_e}{u^2} \frac{F_{3/2}(\alpha^e)}{F_{1/2}(\alpha^e)} + \right.$$
$$\left. + \frac{T_e^2}{u^4} \frac{F_{5/2}(\alpha^e)}{F_{1/2}(\alpha_e)} + \cdots\right)$$
$$- \frac{z^2}{3u^4}\left(1 + \frac{10}{3} \frac{T_e}{u^2} F_{3/2}(\alpha^e)/F_{1/2}(\alpha^e) + \cdots\right) \tag{19}$$

at high frequency ($u \gg a_0(T_e)$), and

$$f_1(u, z) \simeq f_1(0, z) = \frac{T_e^{1/2}}{2} \left(F_{-1/2}(\alpha^e) + \frac{2z^2}{T_e} G_1(\alpha^e)\right),$$
$$= 1 - \frac{z}{3}, \qquad T_e \ll 1$$
$$= \frac{2}{3T_e}\left(1 - \frac{2z}{3T_e}\right), \quad T_e \gg 1 \tag{20}$$

in the low frequency range ($u \ll a_0(T_e)$).

Relations (14) and (19) give us an important parameter : the location of the resonance ($\varepsilon(z_r, u_r) = 0$) at

$$z_r^2 = -\chi^2 f_1(z_r, u_r) \quad \text{and} \quad f_2(z_r, u_r) = 0$$

so $\quad z_r^2 \ll a_0(T_e) \quad$ and $\quad u_r > a_0(T_e)$

$$z_r^2 = \frac{\chi^2}{3u_r^2}\left(1 + T_e \frac{F_{3/2}(\alpha^e)}{u_r^2 F_{1/2}(\alpha^e)} + \frac{T_e^2 F_{5/2}(\alpha^e)}{u_r^2 F_{1/2}(\alpha^e)}\right) \tag{21}$$

3. Born R.P.A. (B.R.P.A.) stopping power.

In dimensionless units (z and u) the B.P.R.A. stopping power

$$S \equiv -\frac{dE}{dx} = \frac{2}{\pi}\left(\frac{ze}{V}\right)^2 \int_0^\infty \frac{dq}{q} \int_0^\infty d\omega\, \omega \,\mathrm{Im}\left(\frac{1}{\varepsilon(q,\omega)}\right) \tag{22}$$

is written in the form

$$\frac{dE}{dx} = \gamma = -\frac{z^2 e^4}{4\pi\varepsilon_0^2 m_e V^2} n_e L_e \tag{23}$$

$$\begin{aligned} L_e &= \frac{6}{\pi\chi^2}\int_0^{V/V_F} u\,du \int_0^\infty z\,dz\,\mathrm{Im}\frac{1}{\varepsilon(z,u)} \\ &= \frac{6}{\pi\chi^2}\int_0^{V/V_F} u\,du \int_0^\infty z^3\,dz \frac{\chi^2 f_2(z,u)}{\{z^2 + \chi^2 f_1(z,u)\}^2 + \{\chi^2 f_2(z,u)\}^2} \end{aligned} \tag{24}$$

with L_e also dimensionless. L_e depends on T_e through $\varepsilon(z, u)$ only.

At this point, we have to make clear a few obvious assumptions.

On most part of their range the projectiles are more energetic than target particles. So, their trajectory may be taken as linear, in view of the very small energy exchange at each encounter. The projectile ions are supposed to be pointlike with a given charge.

Equation (24) is free from divergences at $z \gg a_0(T_e)$, diffraction effects yield $f_2 = 0$, while shielding through $|\varepsilon(z, u)|^2$ secures the opposite limit $z \ll a_0(T_e)$. With R.P.A., one has

$$|\chi^2 f_1|, \quad |\chi^2 f_2| \ll a_0(T_e)$$

and one divides the z-domain into two regions :

— $z \ll a_0(T_e)$, where the test charge yields its energy to the collective modes with a resonance at $z = z_r$ when $u > a_0(T_e)$, and energy exchange close to $\hbar\omega_r \simeq \hbar\omega_p$.

— $|z - u| < a_0(T_e)$, which pertains to binary collisions. For $u > a_0(T_e)$, shielding vanishes. The corresponding energy exchange is now $\hbar\omega = \dfrac{\hbar^2 q^2}{2m}$.

These two domains remain distinct when $u > a_0(T_e)$; i.e. for an energy exchange larger than the kinetic energy $\simeq k_B T_F(1 + T_e)$. This basic property accounts for the weak coupling character of the R.P.A. Collective modes retain less energy than the particle kinetic energy.

Moreover the usual Z^2-dependence of the stopping formula yields the well-known scaling relation

$$\frac{dE'}{dx}(z', M', E') = \frac{z'^2}{z^2}\frac{dE}{dx}\left(z, M, \frac{M}{M'}E'\right)$$

so we restrict to protons in the sequel.

It should be appreciated that one of the main outputs of the present work is the possibility to compute S for any velocity ratio V/V_{th}, because partial degeneracy is treated exactly.

For instance, in the large V limit

$$\frac{V}{a_0(T_e) V_F} \gg 1$$

one may check that, for $T_e \neq 0$, there are, as in the $T_e = 0$ case [8, 9], two equal contributions of S :

— exchange of energy with a plasmon mode around $z \simeq z_r$;

— exchange of energy through binary encounters around $z = u$.

4. Numerical results and approximations.

In order to get orders of magnitude for the most relevant parameters, we put them in numerical correspondence in table I.

The numerical analysis of equation (24) is mostly performed through

$$F(z, u) = -z\,\mathrm{Im}\frac{1}{\varepsilon(z,u)}$$

and

$$\int_0^\infty dz\,F(u,z) = \int_0^{z_1} dz\,F(z,u) + \int_{z_1}^{z_2} dz\,F(z,u) + \int_{z_2}^\infty dz\,F(z,u) \equiv I_1 + I_2 + I_3 \tag{25}$$

with
$$\begin{aligned} &z_1 = z_2 = 0, && u \leqslant a_0(T_e) \\ &z_1 = \mathrm{Max}(0, z_r(u) - \varepsilon) && \\ &z_2 = z_r(u) + \varepsilon, && u > a_0(T_e) \\ &\varepsilon \simeq 0.01\, a_0(T_e) && \end{aligned}$$

Table I. — *Relations between α^e and T_e, and n, x^2 and T_F. α'_e is given by the normalizations condition for the Boltzmann statistics.*

α^e	$-$ 5	$-$ 1.5	0	1.5	5.	
T_e	23.22	2.361	0.9887	0.4973	0.1934	
α'_e	$-$ 5.002	$-$ 1.573	$-$ 0.268	0.763	2.18	
$n\,(\mathrm{cm}^{-3})$	10^{22}	10^{23}	10^{24}	10^{25}	10^{26}	10^{27}
x^2	0.902	0.419	0.194	0.902×10^{-1}	0.419×10^{-1}	0.194×10^{-1}
$T_F\,(\mathrm{K})$	0.196×10^5	0.912×10^5	0.423×10^6	0.196×10^7	0.912×10^7	0.423×10^8

I_1 and I_3 are evaluated numerically, while I_2 can be given an analytic expression. For instance, for

$$\frac{\chi^2}{1 + T_e} \ll 1 \quad \text{and} \quad u \gg a_0(T_e)$$

$$I_2 = \frac{\pi}{2}\, z_r^2(u)\,.$$

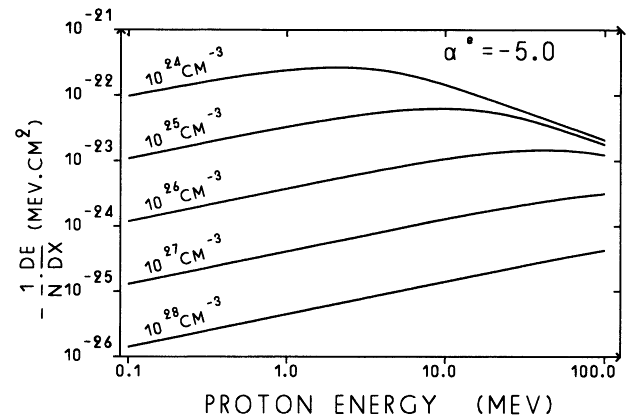

FIG 1.A

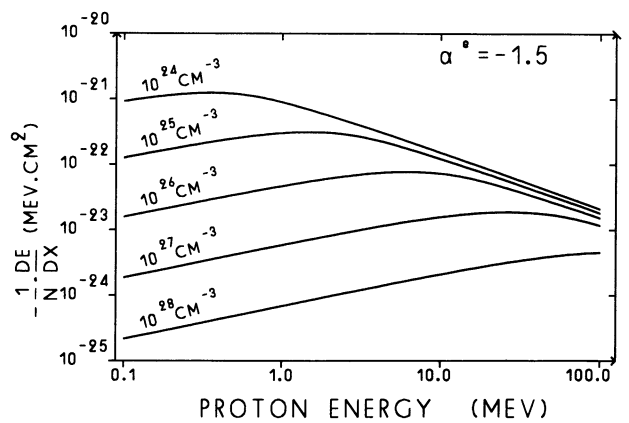

FIG 1.B

Figs. 1a-e. — Stopping power $- \mathrm{d}E/n\,\mathrm{d}x$ (MeV, cm^2) as a function of proton energy E for various electron densities $n = 10^{24}$-$10^{28}\ \mathrm{cm}^{-3}$, and several degeneracy parameters α^e. a) $\alpha^e = 5$, b) $\alpha^e = -1.5$, c) $\alpha^e = 0$, d) $\alpha^e = +1.5$, e) $\alpha^e = 5.0$.

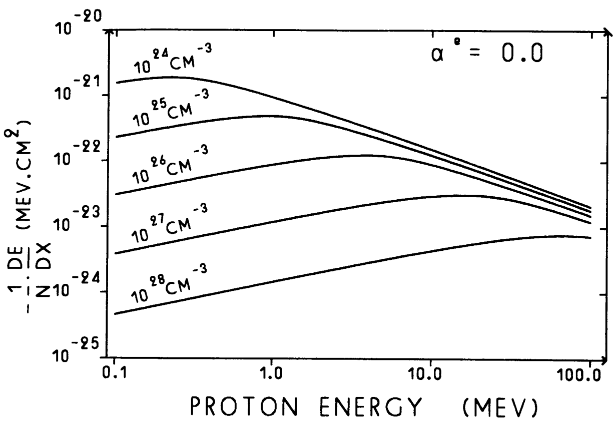

FIG 1.C

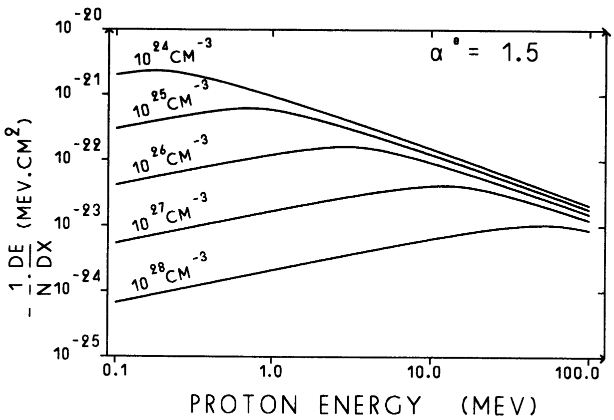

FIG 1.D

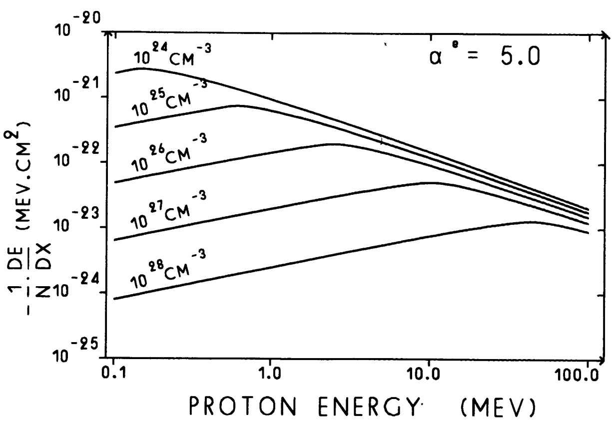

FIG 1.E

$S = -\dfrac{dE}{n\,dx}$ is displayed on figure 1 for various densities n in the target as a function of the projectile (proton) energy, for a given degeneracy parameter α^e. Basic trends are as follows :

— Maximum stopping efficiency is achieved for $V \simeq V_{th}$.

— $\dfrac{dS}{dT} \simeq 0$ for $V \gg V_{th}$

— $S \sim n^{-1}$ for $V \ll V_{th}$

4.1 Low projectile velocity $\left(x = \dfrac{V}{V_{th}} \ll 1\right)$. — Equation (24) then becomes :

$$L_e = \frac{V^3}{V_F}\int_0^\infty \frac{dz\, z^3}{(z^2 + Z_c(z))^2\left(1 + \exp\left[\frac{z^2}{T_e} - \alpha^e\right]\right)} = \left(\frac{V}{V_F}\right)^3 C(\chi^2, \alpha^e) \tag{26}$$

where

$$Z_c(z) = \chi^2 f_1(z, 0)$$

when $\chi^2/(1 + T_e) \ll 1$ we can use the additional assumption :

$$Z_c(z) \simeq \chi^2 f_1(0, 0) = \frac{T_e^{1/2}}{2} F_{1/2}(\alpha^e) = Z_c^2 = \frac{1}{4\, q_F^2\, \lambda_{TF}^2},\ \lambda_{TF}^2 = \frac{V_F^2}{3\,\omega_p^2},\quad \text{Thomas-Fermi}\quad T_e \ll 1$$

$$= \frac{1}{4\, q_F^2\, \lambda_D^2},\ \lambda_D^2 = \frac{k_B\, T}{4\,\pi n e^2},\quad \text{Debye}\quad T_e \gg 1. \tag{27}$$

Equation (27) for Z_c^2 allows to rewrite L_e as

$$L_e = \left(\frac{V}{V_F}\right)^3 \frac{1}{2}\left(\ln\frac{1 + Z_c^2}{Z_c^2} - \frac{1}{1 + Z_c^2}\right),\quad T_e \ll 1$$

$$= \frac{2}{\sqrt{\pi}}\frac{x^3}{3}\ln\frac{1}{4\,\delta e\gamma},\quad T_e \gg 1 \tag{28}$$

where $\gamma = e^{0.517}$, $\delta = \dfrac{\lambda\!\!\!^{-2}}{16\,\lambda_D^2}$, $\lambda\!\!\!^{-} = \dfrac{\hbar}{mV_{th}}$

Approximation (28) is excellent for $\dfrac{\chi^2}{1 + T_e} \ll 1$ and lags within 15 % in a cold solid.

4.2 High projectile velocity ($x \gg 1$). — Extending the $T = 0$ Lindhard-Winther procedure to any temperature we make use of

$$\lim_{V\to\infty}\left\{\int_0^\infty dz \int_0^{V/V_F} du F(u, z)\right\} = \lim_{V\to\infty}\left\{\int_{z_r(V/V_F)}^{V/V_F} dz \int_0^\infty du\, F(u, z)\right\} \tag{29}$$

and

$$\int_0^\infty d\omega\, \omega\, \mathrm{Im}\,\frac{1}{\varepsilon(q, \omega)} = \frac{\omega_p^2}{2} \tag{30}$$

to derive

$$\lim_{V\to\infty} L_e = \int_{z_r(V/V_F)}^{V/V_F} \frac{dz}{z} = \ln\left(\frac{V}{V_F\, z_r\left(\frac{V}{V_F}\right)}\right) \tag{31}$$

which, when combined to equation (23) through

$$\left\langle \frac{V_e^{2n}}{V_F^2} \right\rangle = \frac{T_e^n\, F_{n+1/2}(\alpha^e)}{F_{1/2}(\alpha^e)}$$

yields (m = electron mass)

$$\lim_{V\to\infty} L_e = \ln\frac{2\, mV^2}{\hbar\omega_p} - \frac{\langle V_e^2 \rangle}{V^2} - \left[\frac{\langle V_e^4 \rangle - 0.5\,\langle V_e^2 \rangle^2}{V^4}\right] + \cdots \tag{32}$$

The full V^{-2}-expansions are thus recovered from $L_e(V_1) - L_e(V_2)$ with $V_{1,2} \gg V_{th}$ so that

$$\lim_{V\to\infty} L_e = \ln\frac{2\, mV^2}{\hbar\omega_p} - \frac{\langle V_e^2 \rangle}{V^2} - \frac{\langle V_e^4 \rangle}{2\, V^4} + \cdots, \tag{33}$$

(33) already gives a one percent accuracy for $V > 2\, V_{th}$. The sum rule result (32) lies remarkably close to this full asymptotic one.

4.3 Interpolation formula (any V). — To a large extent, the numerical gap between (33) and (26) (i.e. between low V and high V) can be bridged through

$$L_e(V) = \left(\frac{V}{V_F}\right)^3 C(\chi^2, \alpha^e) \times \frac{1}{(1 + GV^2)} = L_e^1(V),\ V \leqslant V_{int}$$

$$= \ln\left(\frac{2\, mV^2}{\hbar\omega_p}\right) - \frac{\langle V_e^2 \rangle}{V^2} - \frac{\langle V_e^4 \rangle}{2\, V^4} = L_e^2(V),\ V \geqslant V_{int} \tag{34}$$

where G is fixed by $L_e^1(V_{int}) = L_e^2(V_{int})$.

Equation (34) is plotted on figure 2 for

$$V_{int} = \sqrt{1.5 < V_e^2 > + \frac{3\,\hbar\omega_p}{2\, m}},$$

with a relative error (any T) smaller than five percent for $\dfrac{\chi^2}{1 + T_e} < 0.3$.

4.4 Statistical effects. — At this point, we think it worthwhile to investigate quantitative modifications of stopping when one replaces Fermi statistics by

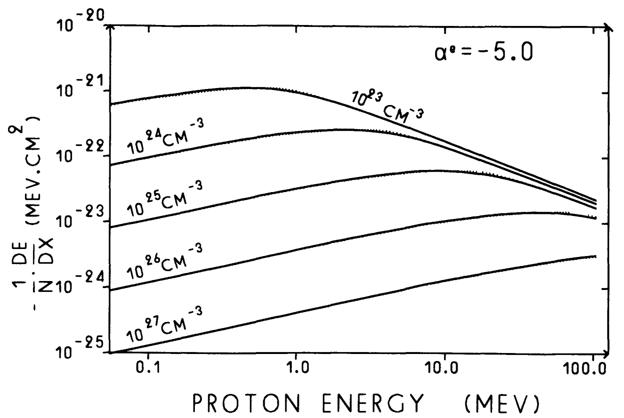

FIG 2.A

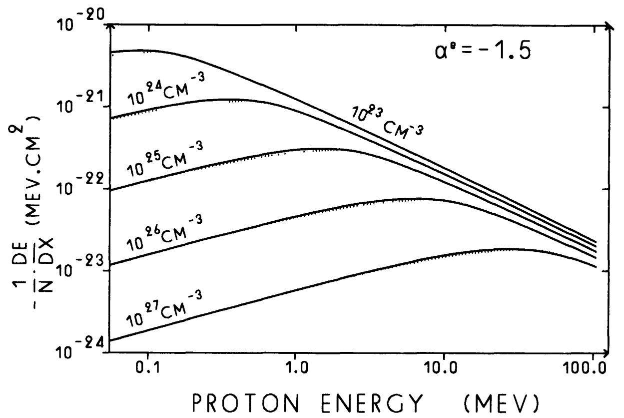

FIG 2.B

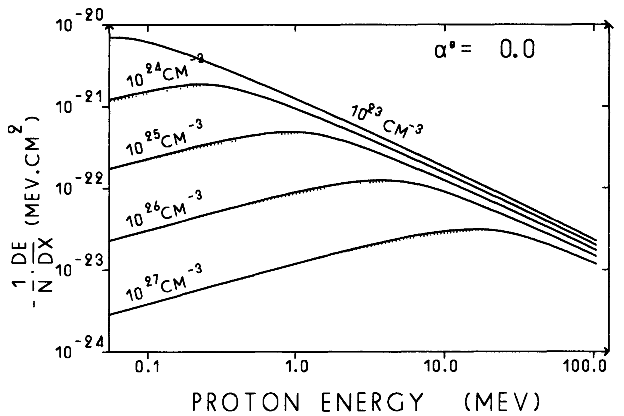

FIG 2.C

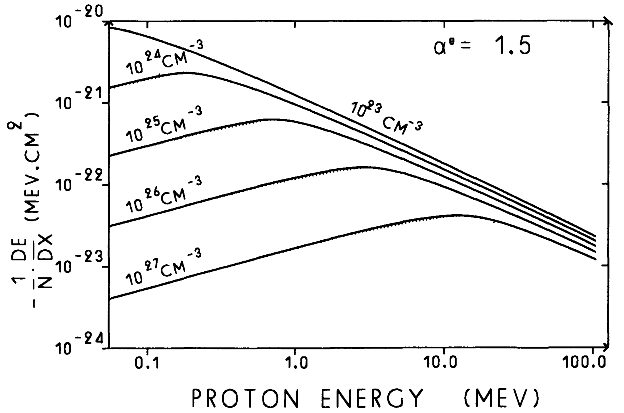

FIG 2.D

Figs. 2a-d. — Same caption as for figure 1 with dotted lines referring to the interpolation formula (34).

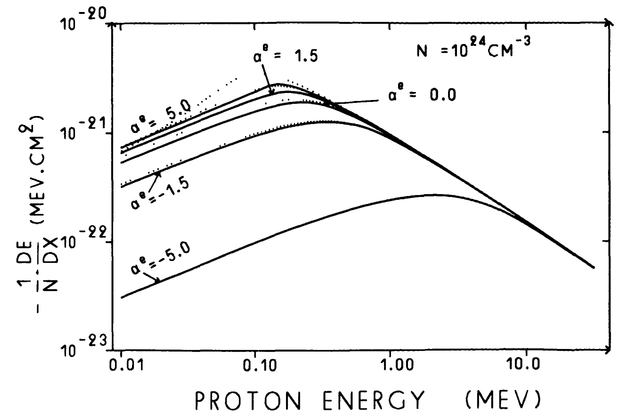

FIG 3.A

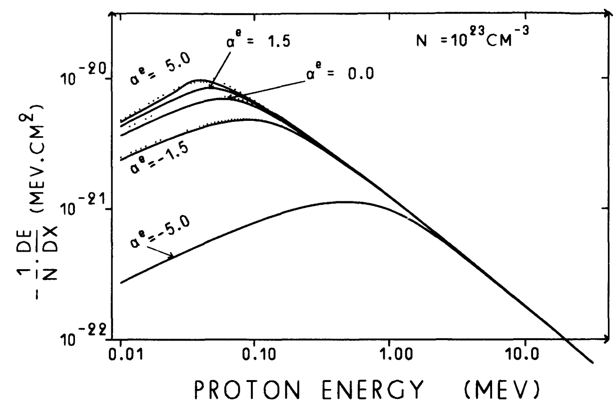

FIG 3.B

Figs. 3a-b. — Comparison of Fermi (full line) and Boltzmann (dotted line) stopping power for same target density and projectile velocity, at various degeneracies.

Boltzmann at an arbitrary temperature. For instance, on figure 3, we compare $\frac{\mathrm{d}E}{\mathrm{d}x}$ respectively computed with a Fermi distribution $f(E) = \left(1 + \mathrm{e}^{\frac{E}{T} - \alpha^{\mathrm{e}}}\right)^{-1}$ and a Boltzmann distribution $f_{\mathrm{B}}(E) = \mathrm{e}^{\alpha'_{\mathrm{e}} - \frac{E}{T}}$ for the same (n, T) data through $F(p) = \frac{4}{3\,\pi T_{\mathrm{e}}^{3/2}}\, Z\!\left(\frac{P}{T_{\mathrm{e}}^{1/2}}\right)$ ($Z(x)$ = Fried-Conte expression) and

$$f_2(z, u) = \frac{\pi T_{\mathrm{e}}}{8\,z}\left(\mathrm{e}^{\alpha'_{\mathrm{e}} - p_-^2/T_{\mathrm{e}}} - \mathrm{e}^{\alpha'_{\mathrm{e}} - p_+^2/T_{\mathrm{e}}}\right) \qquad (35)$$

with α'_{e} plotted on the last line in table I. $\alpha^{\mathrm{e}} = \alpha'_{\mathrm{e}}$ at $T_{\mathrm{e}} \gg 1$.

Moreover, we recover $\frac{\mathrm{d}E}{\mathrm{d}x} = \frac{\mathrm{d}E^{\mathrm{B}}}{\mathrm{d}x}$ at high velocity. Statistical effects are thus mostly significant in the low velocity regime.

— As expected discrepancies increase with increasing α^e. For instance maxima exhibit a 6% discrepancy for $T_e = 1$ and a 12 % one for $T_e = 0.5$ respectively. Also, the maximum and slope of $\frac{dE^B}{dx}$ tend to shift gradually away from their Fermi homologues.

— Fermi statistics gradually freezes out the free electron degrees of freedom, altogether with the corresponding stopping. All in all, a Fermi plasma tends to be more transparent than a Maxwellian one.

However, it should be noted that for low T and V, the classical Debye screening is more efficient than the Thomas-Fermi screening, which reduces $\frac{dE^B}{dx}$.

5. Limit behaviours.

— In view of the obvious fact that previous calculations were essentially restricted to the high- and low-temperature domains, respectively, we consider here these limit behaviours.

5.1 $T \to \infty$. — At high-temperature, we can make a quantitative assessment of the well-known Jackson procedure [2, 15], which essentially consists in a linear superposition of the binary collision theory within a Debye sphere around the projectile in matter with collective plasma oscillations beyond the Debye radius. Within the present formalism, the Jackson limit is retrieved through

$$z = \frac{q\lambda}{2}, u = \frac{\omega}{qV_{\text{th}}}, x = \frac{V}{V_{\text{th}}}$$

and

$$\sqrt{\pi}L_e = \int_0^x du\, u \int_0^\infty dz\, z^2 \frac{[e^{-(u-z)^2} - e^{-(u+z)^2}]}{\left[z^2 - \frac{\delta}{z}(Z(u+z) - Z(u-z))^2 + \left(\frac{\delta}{z}\pi^{1/2}(e^{-(u-z)^2} - e^{-(u+z)^2})\right)^2\right]} \tag{36}$$

from which one gets when $\delta \to 0$

$$L_e = \psi(x)(\ln(\Lambda_F) + \Delta(x)) = L_e^J + \psi(x)\Delta(x) \tag{37}$$

$$\psi(x) = \operatorname{erf}(x) - \frac{2x}{\sqrt{\pi}} e^{-x^2}$$

$$\Lambda_F = \frac{0.764\, x^2}{\sqrt{2\delta}}(1 + x^{-2})^{1/2}.$$

The product $\psi(x)\Delta(x)$ accounts for the discrepancy between the Jackson and R.P.A. results in the $\delta = 0$ limit. Equation (37) easily simplifies at high and low projectile velocities. One thus gets

$$L_e = \ln \frac{2mV^2}{\hbar\omega_p} - \frac{3}{2x^2} - \frac{15}{8x^4}, \quad x \gg 1 \tag{38a}$$

with $\Delta(x) = -\ln(0.764) - \frac{2}{x^2} - \frac{13}{8x^4}$, and

$$L_e = \frac{2}{3\sqrt{\pi}} x^3 \ln\left(\frac{1}{4\delta e\gamma}\right), \quad x \ll 1 \tag{38b}$$

Table II. — *Values of Δ used in table II.*

x	Δ	x	Δ	x	Δ	x	Δ
0.1	1.37	1.5	− 0.565	2.9	-0.166×10^{-1}	4.5	0.150
0.2	0.729	1.6	− 0.526	3.0	$+0.326 \times 10^{-2}$	5.	0.167
0.3	0.365	1.7	− 0.482	3.1	$+0.210 \times 10^{-1}$	5.5	0.185
0.4	0.776×10^{-1}	1.8	− 0.434	3.2	$+0.369 \times 10^{-1}$	6.	0.197
0.5	− 0.133	1.9	− 0.384	3.3	$+0.512 \times 10^{-1}$	6.5	0.213
0.6	− 0.286	2.0	− 0.333	3.4	$+0.641 \times 10^{-1}$	7.	0.227
0.7	− 0.402	2.1	− 0.284	3.5	$+0.758 \times 10^{-1}$	7.5	0.233
0.8	− 0.491	2.2	− 0.238	3.6	$+0.864 \times 10^{-1}$	8.	0.237
0.9	− 0.555	2.3	− 0.195	3.7	$+0.960 \times 10^{-1}$	8.5	0.241
1.0	− 0.597	2.4	− 0.157	3.8	+ 0.105	9.	0.244
1.1	− 0.619	2.5	− 0.122	3.9	+ 0.113	9.5	0.247
1.2	− 0.625	2.6	-0.913×10^{-1}	4.	+ 0.120	10.	0.249
1.3	− 0.617	2.7	-0.636×10^{-1}				
1.4	− 0.596	2.8	-0.388×10^{-1}				

with $2\,\Delta(x) = \ln\left(\frac{1}{e\gamma}\right) - \ln(1.167\,x^2)$ $\Delta(x)$ is plotted in table II. $\Delta(x)$ is connected with Δ_1 and Δ_2 tabulated by May [16] :

$$\Delta(x) = \Delta_1(x) + \frac{1}{2}\Delta_2(x) + \frac{1}{2} - \ln\left(0.764\,x^2\sqrt{1+\frac{1}{x^2}}\right).$$

Again, it is possible to bridge the gap between (38a) and (38b) through

$$L_e^1 = \psi(x)\ln\left(\frac{1}{\sqrt{2\,\delta}}\right)\cdot\frac{x^4 + A}{x^2 + B}, \qquad (39)$$

$$B = 1.5,\ A = 0.482\,.$$

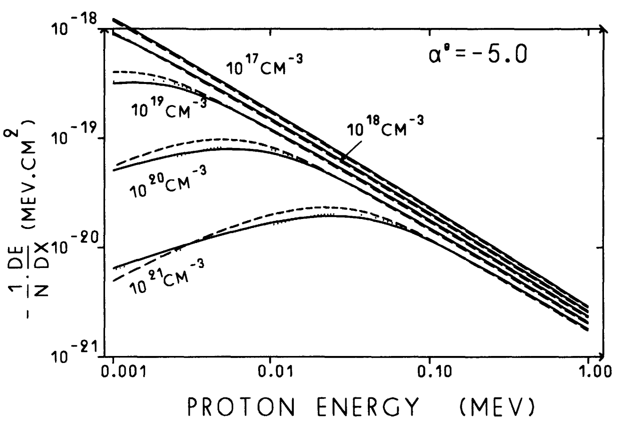

FIG 4.A

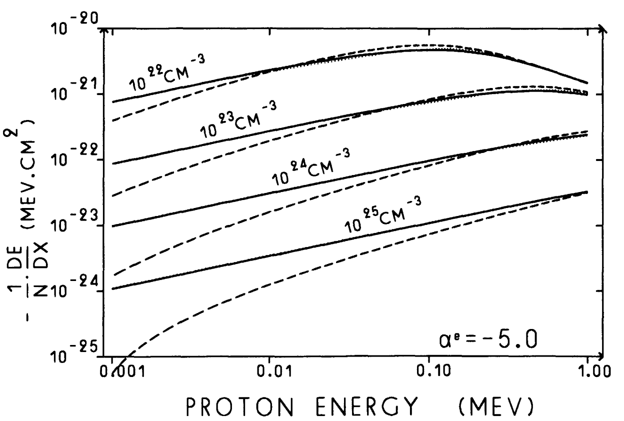

FIG 4.B

Figs. 4a-b. — Comparison of present stopping power (full line) with Jackson approximation (37) (dashed line) and interpolation formula (39) (dotted line).

On figures 4a, b, we compare L_e^J, L_e^1 and L_e. L_e^J exhibits serious discrepancies in the low V limit, at high n. On the other hand, L_e^1 remains very accurate in the whole parameter range.

5.2 $T_e \to 0$. — In the opposite situation of full degeneracy, we make now a connection with a calculation performed by Dar *et al.* [24]. These authors used the $T = 0$ limit, (Lindard) of $\varepsilon(q, \omega)$ to compute cross-sections for the stopping of deuteron beams in very dense electron fluids at various densities.

On figure 5, we retrieve their results, and the checking is performed at best for $E = 1$ MeV, where $-\frac{1}{n}\frac{dE}{dx}$ is equivalent to a cross-section.

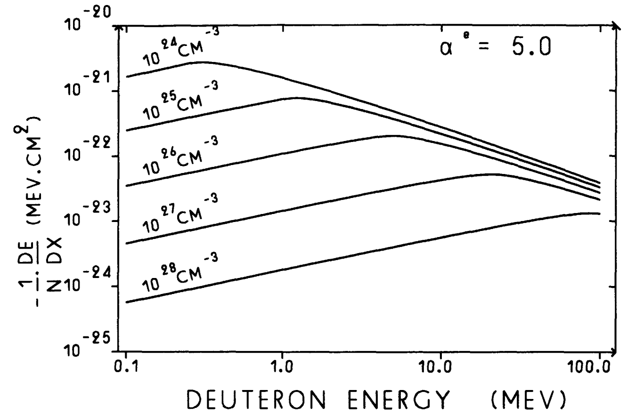

Fig. 5. — Stopping of deuterons in dense electrons. Results of Dar *et al.* [26] are recovered at $E = 1$ MeV.

6. Concluding remarks.

In the above treatment, we have completely worked out the stopping of nonrelativistic and pointlike ions in an arbitrarily degenerate electron fluid, within the theoretical framework provided by the Born approximation for the projectile and R.P.A. for the target plasma (B.R.P.A.).

When the projectile charge Z is such that the Born parameter

$$\frac{ZV_0}{(V^2 + V_{th}^2)^{1/2}} \qquad (40)$$

is no longer small as compared to unity, we have to go beyond the present approximation (referred to as Born I) and include higher-order Born corrections in the usual form :

$$-\frac{dE}{dx} = k\frac{Z^2}{V^2}\left[L_0 + ZL_1 + f(Z^2)\right] \qquad (41)$$

where L_0 denotes the previous B.R.P.A. contribution. ZL_1 is the Born II correction equivalent to a Barkas term [19, 22], $f(Z^2)$ is the Bloch term [23] which bridges the gap between quantum and classical theories. $f(Z^2)$ has been computed in the nondegenerate limit [17, 18].

From (41) one can see that all theories start from the B.R.P.A. results. So our conclusions remain valid in a more general framework than the Born approximation one.

References

[1] ARISTA, N. R. and BRANDT, W., *Phys. Rev.* **A 23** (1981) 1898.
[2] MEHLHORN, Th. A., *J. Appl. Phys.* **52** (1981) 6522.
[3] NARDI, E., PELEG, E. and ZINAMON, Z., *Phys. Fluids* **21** (1978) 574.
[4] SKUPKY, S., *Phys. Rev.* **A 16** (1977) 727.
[5] DEUTSCH, C., MAYNARD, G. and MINOO, H., *Laser Interaction and Related Plasma Phenomena,* Vol. 6, Ed. by H. Hora and G. H. Miley (1984), also DEUTSCH, C., *Laser Partic. Beams* **2** (1984) 449.
[6] MAYNARD, G. and DEUTSCH, C., *Phys. Rev.* **A 26** (1982) 665.
[7] MAYNARD, G., Thèse 3e Cycle, Orsay (1982) (unpublished).
[8] LINDHARD, J., WINTER, A., *Mat. Fys. Medd.* **34** N° 4 (1964).
[9] HARRIS, E. G., in *Advances in Plasma Physics,* Vol. 3 (1969), Ed. by A. Simon and W. B. Thompson.
[10] ARISTA, N. R. and BRANDT, W., *Phys. Rev.* **A 29** (1984) 1471.
[11] GOUEDARD, C. and DEUTSCH, C., *J. Math. Phys.* **19** (1978) 32.
[12] CADY, W. J. and THARKER, H. C., Jr., *Math. Comp.* **21** (1967) 30.
[13] FRIED, B. D. and CONTE, S. D., *The Plasma Dispersion Function* (Academic Press) 1961, New York.
[14] NEMETH, G., ÁG, Á. and PÁRIS, Gy., *J. Math. Phys.* **22** (1981) 1192.
[15] JACKSON, J. D., *Classical Electrodynamics* (Wiley, New York) 1975.
[16] MAY, R. M., *Aust. J. Phys.* **22** (1969) 687.
[17] HONDA, N., *J. Phys. Soc. Japan* **19** (1964) 1201 and 1935.
[18] GEORGES, E. P., OKAMOTO, K., NAKAMURA, Y. and HAMADA, T., *Aust. J. Phys.* **32** (1979) 223.
[19] BARKAS, W. H., DYER, J. W. and HECKMANN, H. H., *Phys. Rev. Lett.* **11** (1963) 26.
[20] JACKSON, J. D. and MACCARTHY, *Phys. Rev.* **B 6** (1972) 4131.
[21] ASHLEY, J. C., RITCHIE, R. H. and BRANDT, W., *Phys. Rev.* **B 5** (1972) 2393.
[22] ESBESSEN, H., Lic. Scient. Thesis, University of Arhus (1977), unpublished.
[23] BLOCH, F., *Ann. Phys.* **16** (1933) 285.
[24] DAR, A., GRUNZWEI-GENOSSAR, J., PERES, A., REVZEN, M. and RON, A., *Phys. Rev. Lett.* **32** (1979) 1299.